COMPLEX DYNAMIC BEHAVIORS OF A DISCRETE-TIME PREDATOR-PREY SYSTEM*

Ming Zhao†, Cuiping Li and Jinliang Wang

Abstract The dynamics of a discrete-time predator-prey system is investigated in detail in this paper. It is shown that the system undergoes flip bifurcation and Hopf bifurcation by using center manifold theorem and bifurcation theory. Furthermore, Marotto's chaos is proved when some certain conditions are satisfied. Numerical simulations are presented not only to illustrate our results with the theoretical analysis, but also to exhibit the complex dynamical behaviors, such as the period-6, 7, 8, 10, 14, 18, 24, 36, 50 orbits, attracting invariant cycles, quasi-periodic orbits, nice chaotic behaviors which appear and disappear suddenly, coexisting chaotic attractors, etc. These results reveal far richer dynamics of the discrete-time predator-prey system. Specifically, we have stabilized the chaotic orbits at an unstable fixed point using the feedback control method.

Keywords Predator-prey system, flip bifurcation, Hopf bifurcation, Marotto's chaos, feedback control.

MSC(2010) 39A28, 39A33, 65P20.

1. Introduction

Predator-prey interaction is always a key issue in mathematical modelling of ecological processes. Considerable progress has been made since the famous Lotka-Volterra predator-prey model was proposed. In recent years, the study of the complex dynamics of the predator-prey models, including aspects as stability, periodic solutions, bifurcations and chaotic behavior, has drawn much attention to many excellent researchers [4–7, 11, 13–15, 17, 25].

The well known predator-prey model due to the mathematician Volterra [26] has the following form:

$$\begin{cases} \dot{x} = ax - bxy, \\ \dot{y} = -cy + dxy, \end{cases}$$

where x and y represent the number of a prey and a predator, respectively, and a, b, c, d are positive parameters. This model considers that, in the absence of predator the number of prey grows exponentially and in the absence of a prey population the number of predator decreases exponentially. This model was changed

by Martelli [23] who considered some harvesting activities as:

$$\begin{cases} \dot{x} = ax - bxy - \gamma x, \\ \dot{y} = -cy + dxy - \gamma y. \end{cases}$$

The author obtained the result that a moderate harvesting activity would favor the prey population. There are also many other predator-prey models of various types that have been extensively investigated and some of the relevant work may be found in [6, 14, 15, 17]. These researches dealing with specific interactions have mainly focused on continuous predator-prey models with two variables.

However, discrete-time models are widely used to understand the complex problem of the competition between two species. For example, the predator-prey models with age-structure for predator are studied in [19], in which they investigated the dynamical complexities including quasi-periodic attractors and strange attractors by using numerical analysis. Recently, bifurcation and chaos in a discrete-time predator-prey system of Holling and Leslie type are investigated in [13]. They gave the conditions under which the system undergoes flip bifurcation and Hopf bifurcation by using the center manifold theorem and the bifurcation theory. The dynamical behaviors including the periodic solutions, bifurcations, chaos for the predator-prey systems as discrete-time models are also investigated in [4,5,7,11,25].

It is noteworthy to mention that in [8], Danca et al. considered the model (1.1) with the prey's growth be governed by a logistic map. The authors investigated local stability conditions of the fixed points in this model, determined the domains of the values of parameters for which the system has stationary states or chaotic behavior. The analysis indicated that the system undergoes Hopf bifurcation. But they only claimed numerical evidence of such bifurcation and chaotic behavior, and they did not theoretically prove the existence of them. Therefore, in this paper we will theoretically prove the existence of bifurcations. And we will also show the existence of Marotto's chaos.

In this paper, we consider the following discrete-time predator-prey system in [8]

$$F : \begin{pmatrix} x \\ y \end{pmatrix} \mapsto \begin{pmatrix} rx(1-x) - bxy \\ dxy \end{pmatrix}, \tag{1.1}$$

where x and y represent population densities of a prey and a predator, respectively, at time t, and r, b, d are positive parameters. Here, $rx(1-x)$ stands for the rate of increase of the prey population in the absence of predators, while the terms $-bxy$ and dxy describe the predator-prey encounters which are favorable to predators and fatal to prey, where b and d are the predation parameters.

Our main motivation in this paper is to investigate the system (1.1) in detail. Here, we derive the conditions of existence for flip bifurcation and Hopf bifurcation by using bifurcation theory and center manifold theorem [12, 27]. The existence of chaos in the sense of Marotto [20, 21] is proved by using both analytical and numerical methods. Numerical simulations, including bifurcation diagrams, phase portraits, maximum Lyapunov exponents and fractal dimension [1, 2, 16, 24], are used to verify the theoretical analysis and to display new and interesting dynamical behaviors of the system (1.1). More specifically, this paper presents the period-6, 7, 8, 10, 14, 18, 24, 36, 50 orbits, attracting invariant cycles, quasi-periodic

orbits, the chaotic sets, nice chaotic behaviors which appear and disappear suddenly, interior crisis phenomena, and the new nice types of five and six coexisting chaotic attractors. In particular, we observe that when the prey is in chaotic dynamic, the predator can tend to extinction or to a stable fixed point. The computations of Lyapunov exponents confirm the dynamical behaviors. The analysis and results are interesting in mathematics and biology. Moreover, these results could be useful when the local and global stabilities in discrete-time predator-prey systems are concerned.

This paper is organized as follows: In section 2, we show the existence and stability of fixed points. In section 3, the sufficient conditions on the existence of codimension-one bifurcations, including flip bifurcation and Hopf bifurcations are obtained. In section 4, conditions on the existence of Marotto's chaos are given. In section 5, numerical simulation results are presented to support the theoretical analysis and they exhibit new and rich dynamical behaviors. In section 6, chaos is controlled to an unstable fixed point using the feedback control method. A brief conclusion is given in section 7.

2. Existence and Stability of Fixed Points

It is clear that the fixed points of system (1.1) satisfy the following equations:

$$\begin{cases} rx(1-x) - bxy = x, \\ dxy = y. \end{cases}$$

By a simple analysis, it is easy to see that the system (1.1) has one extinction fixed point $(0,0)$, one exclusion fixed point $(\frac{r-1}{r}, 0)$, and one coexistence(positive) fixed point $(x^*, y^*) = (\frac{1}{d}, \frac{rd-r-d}{bd})$. Now we study the stability of these fixed points.

For the fixed point $(0,0)$, the corresponding characteristic equation is $\lambda^2 - r\lambda = 0$ and its roots are $\lambda_1 = 0$, $\lambda_2 = r$ that means $(0,0)$ is asymptotically stable when $0 < r < 1$ and it is unstable when $r > 1$.

For the exclusion fixed point $(\frac{r-1}{r}, 0)$ when $r > 1$. Linearizing the system (1.1) about $(\frac{r-1}{r}, 0)$, we have the following coefficient matrix:

$$J_0 = \begin{pmatrix} 2 - r & -\frac{b(r-1)}{r} \\ 0 & \frac{d(r-1)}{r} \end{pmatrix}.$$

Clearly, J_0 has characteristic roots $\lambda_1 = 2 - r$, $\lambda_2 = \frac{d(r-1)}{r}$. $|\lambda_i| < 1$ $(i = 1, 2)$ holds if and only if

$$1 < r < 3 \quad \text{and} \quad 0 < d < \frac{r}{r-1}.$$

Below we will prove that when $r = 3$ the exclusion fixed point $(\frac{r-1}{r}, 0)$ is asymptotically stable and when $d = \frac{r}{r-1}$ it is unstable by using center manifold theory.

Let $u = x - \frac{r-1}{r}$ and $v = y$ in (1.1), we have

$$\begin{pmatrix} u \\ v \end{pmatrix} \mapsto \begin{pmatrix} (2-r)u + \frac{(1-r)b}{r}v - ru^2 - buv \\ \frac{(r-1)d}{r}v + duv \end{pmatrix}. \tag{2.1}$$

Now we consider the first case, i.e., $r = 3$ and $0 < d < \frac{3}{2}$. The system (2.1) becomes

$$\begin{pmatrix} u \\ v \end{pmatrix} \mapsto \begin{pmatrix} -1 - \frac{2b}{3} \\ 0 \quad \frac{2d}{3} \end{pmatrix} \begin{pmatrix} u \\ v \end{pmatrix} + \begin{pmatrix} -3u^2 - buv \\ duv \end{pmatrix}. \tag{2.2}$$

We construct an invertible matrix

$$T = \begin{pmatrix} 1 & -\frac{2b}{3+2d} \\ 0 & 1 \end{pmatrix},$$

and use the translation

$$\begin{pmatrix} u \\ v \end{pmatrix} = T \begin{pmatrix} X \\ Y \end{pmatrix},$$

then the map (2.2) can be written as:

$$\begin{pmatrix} X \\ Y \end{pmatrix} \mapsto \begin{pmatrix} -1 & 0 \\ 0 & \frac{2d}{3} \end{pmatrix} \begin{pmatrix} X \\ Y \end{pmatrix} + \begin{pmatrix} \tilde{f}(X,Y) \\ \tilde{g}(X,Y) \end{pmatrix}, \tag{2.3}$$

where $\tilde{f}(X,Y) = -3X^2 + \frac{9b}{3+2d}XY - \frac{6b^2}{(3+2d)^2}Y^2$ and $\tilde{g}(X,Y) = dXY - \frac{2bd}{3+2d}Y^2$.

Assume a center manifold with the form $Y = h(X) = \tilde{\alpha}X^2 + \tilde{\beta}X^3 + O(|X|^4)$, then it must satisfy

$$h(-X + \tilde{f}(X, h(X))) - \frac{2d}{3}h(X) - \tilde{g}(X, h(X)) = 0.$$

By the approximate computation for center manifold, we obtain $\tilde{\alpha} = 0$ and $\tilde{\beta} = 0$. Hence $h(X) = 0$, on the center manifold $Y = 0$, the new map $\hat{f}$ is give by

$$\hat{f} = -X + \tilde{f}(X, h(X)) = -X - 3X^2.$$

Some computations show that the Schwarzian derivative of this map at $X = 0$ is $S(\hat{f}(0)) = -54 < 0$. Hence, by [10], the exclusion fixed point $(\frac{r-1}{r}, 0)$ is asymptotically stable.

Next we consider the second case, i.e., $1 < r < 3$ and $d = \frac{r}{r-1}$. The system (2.1) becomes

$$\begin{pmatrix} u \\ v \end{pmatrix} \mapsto \begin{pmatrix} 2 - r & -\frac{(r-1)b}{r} \\ 0 & 1 \end{pmatrix} \begin{pmatrix} u \\ v \end{pmatrix} + \begin{pmatrix} -ru^2 - buv \\ \frac{r}{r-1}uv \end{pmatrix}. \tag{2.4}$$

We construct an invertible matrix

$$T = \begin{pmatrix} 1 & -\frac{b}{r} \\ 0 & 1 \end{pmatrix},$$

and use the translation

$$\begin{pmatrix} u \\ v \end{pmatrix} = T \begin{pmatrix} X \\ Y \end{pmatrix},$$

then the map (2.4) becomes

$$\begin{pmatrix} X \\ Y \end{pmatrix} \mapsto \begin{pmatrix} 2-r & 0 \\ 0 & 1 \end{pmatrix} \begin{pmatrix} X \\ Y \end{pmatrix} + \begin{pmatrix} \tilde{\tilde{f}}(X,Y) \\ \tilde{\tilde{g}}(X,Y) \end{pmatrix}, \tag{2.5}$$

where $\tilde{\tilde{f}}(X,Y) = -rX^2 + \frac{rb}{r-1}XY - \frac{b^2}{r(r-1)}Y^2$ and $\tilde{\tilde{g}}(X,Y) = \frac{r}{r-1}XY - \frac{b}{r-1}Y^2$.

Assume a center manifold with the form $X = h(Y) = \tilde{\tilde{\alpha}}Y^2 + \tilde{\tilde{\beta}}Y^3 + O(|Y|^4)$, then it must satisfy

$$h(Y + \tilde{\tilde{g}}(h(Y),Y)) - (2-r)h(Y) - \tilde{\tilde{f}}(h(Y),Y)) = 0.$$

By the approximate computation for center manifold, we obtain $\tilde{\tilde{\alpha}} = -\frac{b^2}{r(r-1)^2}$ and $\tilde{\tilde{\beta}} = -\frac{(2+r)b^3}{r(r-1)^4}$. Hence $h(Y) = -\frac{b^2}{r(r-1)^2}Y^2 - \frac{(2+r)b^3}{r(r-1)^4}Y^3 + O(|Y|^4)$, on the center manifold $X = h(Y)$, the new map $\hat{\hat{f}}$ is give by

$$\hat{\hat{f}} = Y + \tilde{\tilde{g}}(h(Y),Y) = Y - \frac{b}{r-1}Y^2 - \frac{b^2}{(r-1)^3}Y^3 + O(|Y|^4).$$

Computations show that $\hat{\hat{f}}'(0) = 1$ and $\hat{\hat{f}}''(0) = -\frac{2b}{r-1} < 0$. Hence, by [10], the exclusion fixed point $(\frac{r-1}{r}, 0)$ is unstable. More precisely, it is a semi-stable fixed point from the right.

Therefore, $(\frac{r-1}{r}, 0)$ is asymptotically stable when $1 < r \leq 3$ and $0 < d < \frac{r}{r-1}$.

Finally, we consider the coexistence fixed point $(x^*, y^*) = (\frac{1}{d}, \frac{rd-r-d}{bd})$ for $d > \frac{r}{r-1}(r > 1)$. The Jacobian evaluated at the fixed point (x^*, y^*) is given by

$$J^* = \begin{pmatrix} \frac{d-r}{d} & -\frac{b}{d} \\ \frac{rd-r-d}{b} & 1 \end{pmatrix},$$

and the characteristic equation of the Jacobian matrix J^* can be written as:

$$P^*(\lambda) = \lambda^2 - (\operatorname{tr} J^*)\lambda + \det J^* = \lambda^2 - \frac{2d-r}{d}\lambda + \frac{r(d-2)}{d} = 0. \tag{2.6}$$

According to the *Jury conditions* [22], in order to find the asymptotically stable region of (x^*, y^*), we need to find the region that satisfies the following conditions:

$$P^*(1) > 0, \quad P^*(-1) > 0 \quad \text{and} \quad \det J^* < 1.$$

Since $P^*(1) = \frac{rd-r-d}{d}$, $P^*(-1) = \frac{rd+3d-3r}{d}$, $\det J^* = \frac{(d-2)r}{d}$, then from the relations $P^*(1) > 0$, $P^*(-1) > 0$ and $\det J^* < 1$, we have that

$$1 < r \leq 3, \quad \frac{r}{r-1} < d < \frac{2r}{r-1} \quad \text{or} \quad 3 < r < 9, \quad \frac{3r}{3+r} < d < \frac{2r}{r-1}.$$

We now summarize the above analysis in the following result.

Proposition 2.1. *For the predator-prey system (1.1), the following statements are true:*

(1) $(0,0)$ *is asymptotically stable if* $0 < r < 1$;

(2) $(\frac{r-1}{r}, 0)$ *is asymptotically stable if* $1 < r \leq 3$ *and* $0 < d < \frac{r}{r-1}$;

(3) $(\frac{1}{d}, \frac{rd-r-d}{bd})$ *is asymptotically stable if and only if one of the following conditions holds:*

    (i) $1 < r \leq 3$ *and* $\frac{r}{r-1} < d < \frac{2r}{r-1}$;

    (ii) $3 < r < 9$ *and* $\frac{3r}{3+r} < d < \frac{2r}{r-1}$.

3. Bifurcations

In this section, we mainly focus on the flip bifurcation and Hopf bifurcation of the coexistence fixed point (x^*, y^*). We choose parameter d as a bifurcation parameter for analyzing the flip bifurcation and Hopf bifurcation of (x^*, y^*) by using the center manifold theorem and bifurcation theory of [12, 27].

First we consider the flip bifurcation of system (1.1).

If $d^* = \frac{3r}{r+3}$, then the eigenvalues of the fixed point (x^*, y^*) are $\lambda_1 = -1$ and $\lambda_2 = \frac{6-r}{3}$. We require $|\lambda_2| \neq 1$, thus $r \neq 3$ and $r \neq 9$. In addition, note that the existence of the coexistence fixed point is assured by the relation $d > \frac{r}{r-1}$, so, we get $r > 3$. Hence, we assume that $r > 3$ and $r \neq 9$ in the following discussion.

Let $u = x - x^*$, $v = y - y^*$ and $\bar{d} = d - d^*$, we transform the fixed point (x^*, y^*) of system (1.1) to the origin, and take $\bar{d}$ as a new dependent variable, then system (1.1) becomes

$$\begin{pmatrix} u \\ \bar{d} \\ v \end{pmatrix} \mapsto \begin{pmatrix} -\frac{r}{3} & 0 & -\frac{(r+3)b}{3r} \\ 0 & 1 & 0 \\ \frac{2(r-3)r}{(r+3)b} & \frac{2(r^2-9)}{9rb} & 1 \end{pmatrix} \begin{pmatrix} u \\ \bar{d} \\ v \end{pmatrix} + \begin{pmatrix} f_1(u, \bar{d}, v) \\ 0 \\ f_2(u, \bar{d}, v) \end{pmatrix}, \qquad (3.1)$$

where $f_1(u, \bar{d}, v) = -ru^2 - buv$ and $f_2(u, \bar{d}, v) = \frac{3r}{r+3}uv + \frac{2(r-3)}{3b}u\bar{d} + \frac{r+3}{3r}v\bar{d} + uv\bar{d}$.

We construct an invertible matrix

$$T = \begin{pmatrix} -\frac{(3+r)b}{(r-3)r} & -\frac{b}{r} & -\frac{(r+3)b}{6r} \\ 0 & \frac{9rb}{(r+3)^2} & 0 \\ 1 & 1 & 1 \end{pmatrix},$$

and use the translation

$$\begin{pmatrix} u \\ \bar{d} \\ v \end{pmatrix} = T \begin{pmatrix} X \\ \mu \\ Y \end{pmatrix},$$

then the map (3.1) can be written as:

$$\begin{pmatrix} X \\ \mu \\ Y \end{pmatrix} \mapsto \begin{pmatrix} -1 & 0 & 0 \\ 0 & 1 & 0 \\ 0 & 0 & \frac{6-r}{3} \end{pmatrix} \begin{pmatrix} X \\ \mu \\ Y \end{pmatrix} + \begin{pmatrix} F_1(X, \mu, Y) \\ 0 \\ F_2(X, \mu, Y) \end{pmatrix}, \qquad (3.2)$$

where

$$F_1(X,\mu,Y) = -\frac{3(r+9)b}{(r-9)(r-3)}X^2 - \frac{3(r+3)b}{2(r-9)}XY - \frac{(r-3)rb}{6(r-9)}Y^2 - \frac{9b}{r-9}X\mu$$

$$-\frac{(27-24r+5r^2)b}{2(r-9)(r+3)}Y\mu - \frac{6(r-3)^2b}{(r-9)(r+3)^2}\mu^2 - \frac{3b^2}{2(r-9)}XY\mu$$

$$-\frac{9b^2}{(r-9)(3+r)}X^2\mu - \frac{3(r-3)b^2}{2(r-9)(r+3)}Y^2\mu - \frac{18rb^2}{(r-9)(r+3)^2}X\mu^2$$

$$-\frac{3(r-3)(r+9)b^2}{2(r-9)(r+3)^2}Y\mu^2 - \frac{9(r-3)b^2}{(r-9)(r+3)^2}\mu^3,$$

$$F_2(X,\mu,Y) = \frac{54b}{(r-9)(r-3)}X^2 + \frac{(r+3)rb}{(r-9)(r-3)}XY + \frac{(r^2-6r+27)b}{6(r-9)}Y^2$$

$$+\frac{18(5r-9)b}{(r-9)(r^2-9)}X\mu + \frac{rb}{r-9}Y\mu + \frac{36(r-3)b}{(r-9)(r+3)^2}\mu^2$$

$$+\frac{9b^2}{(r-9)(r-3)}XY\mu + \frac{54b^2}{(r-9)(r^2-9)}X^2\mu + \frac{9b^2}{(r-9)(r+3)}Y^2\mu$$

$$+\frac{108rb^2}{(r-9)(r-3)(r+3)^2}X\mu^2 + \frac{9(9+r)b^2}{(r-9)(r+3)^2}Y\mu^2 + \frac{54b^2\mu^3}{(r-9)(r+3)^2}.$$

By the center manifold theorem, the stability of $(X,Y)=(0,0)$ near $\mu=0$ can be determined by studying a one-parameter family of maps on a center manifold, which can be written as:

$$W^c(0) = \{(X,\mu,Y) \in R^3|\ Y = h^*(X,\mu),\ h^*(0,0)=0,\ Dh^*(0,0)=0\}.$$

Assume

$$h^*(X,\mu) = \alpha X^2 + \beta X\mu + \gamma\mu^2 + O((|X|+|\mu|)^3),$$

by the approximate computation for center manifold, we obtain

$$\alpha = \frac{162b}{(r-9)(r-3)^2},\ \beta = \frac{54b(5r-9)}{(r-3)(r+3)(r-9)^2},\ \gamma = \frac{108b}{(r-9)(r+3)^2}.$$

Therefore, the map restricted to the center manifold is given by

$$\tilde{F}: X \to -X + h_1X^2 + h_2X\mu + h_3\mu^2 + h_4X^3 + h_5X^2\mu + h_6X\mu^2 + h_7\mu^3 + O((|X|+|\mu|)^4),$$

where

$$h_1 = -\frac{3(r+9)b}{(r-3)(r-9)}, \qquad h_2 = -\frac{9b}{(r-9)},$$

$$h_3 = -\frac{6(r-3)^2b}{(r-9)(r+3)^2}, \qquad h_4 = -\frac{243(r+3)b^2}{(r-3)^2(r-9)^2},$$

$$h_5 = -\frac{9(r^2+72r-81)b^2}{(r+3)(r-9)^3}, \quad h_6 = -\frac{9(2r^3+57r^2-216r-243)b^2}{(r+3)^2(r-9)^3},$$

$$h_7 = -\frac{9(r+27)(r-3)^2b^2}{(r-9)^2(r+3)^3}.$$

If map (3.2) undergoes a flip bifurcation, then it must satisfy the following conditions

$$\alpha_1 = [\frac{\partial F}{\partial \mu} \cdot \frac{\partial^2 F}{\partial X^2} + 2\frac{\partial^2 F}{\partial X\partial \mu}]|_{(0,0)} \neq 0,$$

and

$$\alpha_2 = [\frac{1}{2} \cdot (\frac{\partial^2 F}{\partial X^2})^2 + \frac{1}{3} \cdot \frac{\partial^3 F}{\partial X^3}]|_{(0,0)} \neq 0.$$

By a simple calculation, we obtain

$$\alpha_1 = \frac{18b}{9-r} \neq 0 \text{ for } b > 0, \ r > 3 \text{ and } r \neq 9,$$

and

$$\alpha_2 = \frac{18rb^2}{(r-9)(r-3)^2} \neq 0 \text{ for } b > 0, \ r > 3 \text{ and } r \neq 9.$$

It is easy to check that if $3 < r < 9$, then $|\lambda_2| < 1$ and $\alpha_2 < 0$. From the above analysis, we have the following result.

Theorem 3.1. *The system (1.1) undergoes a flip bifurcation at (x^*, y^*) if the following conditions are satisfied: $b > 0$, $r > 3$, $r \neq 9$, and $d = \frac{3r}{r+3}$. Moreover, if $3 < r < 9$, then period-2 points that bifurcate from this fixed point are unstable.*

Next we give the conditions of existence for Hopf bifurcation.

The characteristic equation associated with the linearized system (1.1) at the fixed point $(x^*(d), y^*(d))$ is given by

$$\lambda^2 + p(d)\lambda + q(d) = 0. \tag{3.3}$$

The eigenvalues of the characteristic equation (3.3) are given as

$$\lambda_{1,2}(d) = \frac{-p(d) \pm \sqrt{p(d)^2 - 4q(d)}}{2},$$

where $p(d) = -r + 2rx^* + by^* - dx^*$ and $q(d) = rdx^* - 2rdx^{*2}$.

The eigenvalues $\lambda_{1,2}(d)$ are complex conjugates for $p(d)^2 - 4q(d) < 0$, which leads to

$$d > \frac{r}{2(\sqrt{r}-1)}. \tag{3.4}$$

Let

$$\bar{d}^* = \frac{2r}{r-1}, \quad \text{for } 1 < r < 9. \tag{3.5}$$

We get $q(d^*) = 1$ and $\lambda_{1,2}(d^*) = \frac{5-r}{4} \pm \frac{i\sqrt{10r-9-r^2}}{4} = \rho \pm i\omega$. Under the conditions of (3.4) and (3.5), we have

$$|\lambda_{1,2}(d)| = (q(d))^{\frac{1}{2}} \quad \text{and} \quad d_1 = \frac{d|\lambda_{1,2}(d)|}{dd}|_{d=\bar{d}^*} = \frac{(r-1)^2}{4r} \neq 0.$$

In addition, if $p(\bar{d}^*) \neq 0, 1$, which leads to

$$r \neq 5 \quad \text{and} \quad r \neq 7,$$

then we obtain that $\lambda_{1,2}^n(\bar{d}^*) \neq 1 (n = 1, 2, 3, 4)$.

Let $u = x - x^*$ and $v = y - y^*$. The system (1.1) becomes

$$\begin{pmatrix} u \\ v \end{pmatrix} \mapsto \begin{pmatrix} \frac{3-r}{2} & \frac{(1-r)b}{2r} \\ \frac{r}{b} & 1 \end{pmatrix} \begin{pmatrix} u \\ v \end{pmatrix} + \begin{pmatrix} f_1(u, v) \\ f_2(u, v) \end{pmatrix}, \tag{3.6}$$

where $f_1(u, v) = -ru^2 - buv$ and $f_2(u, v) = \frac{2r}{r-1}uv$.

Let

$$T = \begin{pmatrix} -\frac{\sqrt{10r-9-r^2}b}{4r} & -\frac{(r-1)b}{4r} \\ 0 & 1 \end{pmatrix},$$

and use the translation

$$\begin{pmatrix} u \\ v \end{pmatrix} = T \begin{pmatrix} X \\ Y \end{pmatrix},$$

then the map (3.6) becomes

$$\begin{pmatrix} X \\ Y \end{pmatrix} \mapsto \begin{pmatrix} \rho & -\omega \\ \omega & \rho \end{pmatrix} \begin{pmatrix} X \\ Y \end{pmatrix} + \begin{pmatrix} F_1(X, Y) \\ F_2(X, Y) \end{pmatrix}, \tag{3.7}$$

where $F_1(X, Y) = \frac{b\sqrt{10r-9-r^2}}{4r}X^2 + \frac{b}{2r}XY - \frac{b(r^2-1)}{4r\sqrt{10r-9-r^2}}Y^2$ and $F_2(X, Y) = -\frac{b}{2}Y^2 - \frac{b\sqrt{10r-9-r^2}}{2(r-1)}XY$.

Notice that (3.7) is exactly in the form on the center manifold, in which the coefficient k [12] is given by

$$k = -Re[\frac{(1-2\lambda)\bar{\lambda}^2}{1-\lambda}\xi_{11}\xi_{20}] - \frac{1}{2}|\xi_{11}|^2 - |\xi_{02}|^2 + Re(\bar{\lambda}\xi_{21}),$$

where

$$\xi_{20} = \frac{1}{8}[(F_{1XX} - F_{1YY} + 2F_{2XY}) + i(F_{2XX} - F_{2YY} - 2F_{1XY})],$$

$$\xi_{11} = \frac{1}{4}[(F_{1XX} + F_{1YY}) + i(F_{2XX} + F_{2YY})],$$

$$\xi_{02} = \frac{1}{8}[(F_{1XX} - F_{1YY} - 2F_{2XY}) + i(F_{2XX} - F_{2YY} + 2F_{1XY})],$$

$$\xi_{21} = \frac{1}{16}[(F_{1XXX} + F_{1XYY} + F_{2XXY} + F_{2YYY})$$
$$+ i(F_{2XXX} + F_{2XYY} - F_{1XXY} - F_{1YYY})].$$

Thus, some complicated calculation gives

$$k = -\frac{(3 + 6r + 12r^2 - 6r^3 + r^4)b^2}{64(r-1)} < 0 \ \text{ for } \ 1 < r < 9.$$

From the above analysis, we have the theorem stated as follows.

Theorem 3.2. *The system (1.1) undergoes a Hopf bifurcation at the fixed point $z(x^*, y^*)$ if the following conditions are satisfied: $b > 0$, $1 < r < 9$, $r \neq 5$, 7, and $d = \bar{d}^* = \frac{2r}{r-1}$. Moreover, $k < 0$, thus an attracting invariant closed curve bifurcates from the fixed point for $d > \bar{d}^*$.*

4. Existence of Marotto's chaos

In this section, we rigorously prove that the system (1.1) possesses a chaotic behavior in the sense of Marotto's definition (see [21], [20]) and present the conditions for the existence of chaotic phenomena.

We first give the conditions under which the fixed point $z_0(x^*, y^*)$ of system (1.1) is a snap-back repeller. The eigenvalues associated with the fixed point $z_0(x^*, y^*)$ are given by

$$\lambda_{1,2} = \frac{-p(x^*, y^*) \pm \sqrt{p(x^*, y^*)^2 - 4q(x^*, y^*)}}{2},$$

where $p(x^*, y^*) = -r + 2rx^* + by^* - dx^*$ and $q(x^*, y^*) = rdx^* - 2rdx^{*2}$.

Suppose that the eigenvalues associated with the fixed point z_0 are a pair of complex conjugates with norms exceed 1, which are equivalent to

$$\begin{cases} \dfrac{(r + 2d)^2 - 4rd^2}{d^2} < 0, \\ \dfrac{(d - 2)r - d}{d} > 0, \end{cases}$$

thus, we obtain that $d > \max\{\frac{2r}{r-1}, \frac{r}{2(\sqrt{r}-1)}\}$, where $r > 1$.

Next we need to find a neighborhood $U_r(z_0)$ of $z_0(x^*, y^*)$ in which the norms of eigenvalues exceed 1 for all $(x, y) \in U_r(z_0)$. This is equivalent to the conditions

$$\begin{cases} p(x, y)^2 - 4q(x, y) < 0, \\ q(x, y) - 1 > 0. \end{cases}$$

Let

$$\begin{aligned} S_1(x, y) =& p(x, y)^2 - 4q(x, y) \\ =& b^2 y^2 + (-2rb + (4rb - 2bd)x)y + (4r^2 + 4rd + d^2)x^2 - (4r^2 + 2rd)x + r^2. \end{aligned}$$

If $\triangle_1 = rdx - 2rdx^2 \geq 0$, i.e., $0 \leq x \leq \frac{1}{2}$, the equation $S_1(x, y) = 0$ has two positive roots denoted as

$$\bar{y}_1 = \frac{r + dx - 2rx - 2\sqrt{rdx - 2rdx^2}}{b}, \quad \bar{y}_2 = \frac{r + dx - 2rx + 2\sqrt{rdx - 2rdx^2}}{b}.$$

Thus, $S_1(x, y) < 0$ if $x \in D_1 = \{x \mid 0 < x < \frac{1}{2}\}$ and $y \in D_3 = (\bar{y}_1, \bar{y}_2)$.

Let

$$S_2(x, y) = q(x, y) - 1 = -2rdx^2 + rdx - 1.$$

If $\triangle_2 = rd(rd - 8) \geq 0$, i.e., $rd > 8$, then the equation $S_2(x, y) = 0$ has two positive roots denoted as

$$\bar{x}_1 = \frac{1}{4} - \frac{1}{4}\sqrt{\frac{rd - 8}{rd}}, \quad \bar{x}_2 = \frac{1}{4} + \frac{1}{4}\sqrt{\frac{rd - 8}{rd}}.$$

Therefore, $S_2(x, y) > 0$ if $x \in D_2 = \{x \mid \bar{x}_1 < x < \bar{x}_2\}$, $y \in R$, and $rd > 8$.

These conditions $b > 0$, $r > 1$, $d > 1$, $rd > 8$, and $d > \max\{\frac{2r}{r-1}, \frac{r}{2(\sqrt{r}-1)}\}$ are equivalent to $b > 0$, $1 < r < 9$, $d > \frac{2r}{r-1}$ or $b > 0$, $r > 9$, $d > \frac{r}{2(\sqrt{r}-1)}$. Thus, we have the following result.

Lemma 4.1. *Let $b > 0$, $1 < r < 9$, $d > \frac{2r}{r-1}$ or $b > 0$, $r > 9$, $d > \frac{r}{2(\sqrt{r}-1)}$, if the following conditions are satisfied:*

$$x \in D_2 = D_1 \cap D_2 \quad and \quad y \in D_3,$$

then $p(x,y)^2 - 4q(x,y) < 0$ and $q(x,y) - 1 > 0$. Moveover, if the fixed point $z_0(x^*, y^*)$ of system (1.1) satisfies

$$z_0(x^*, y^*) \in U_r(z_0) = \{(x,y) | x \in D_2, \ y \in D_3\},$$

then $z_0(x^*, y^*)$ is an expanding fixed point in $U_r(z_0)$.

According to the definition of snap-back repeller, one also needs to find one point $z_1(x_1, y_1) \in U_r(z_0)$ such that $z_1 \neq z_0$, $F^M(z_1) = z_0$ and $|DF^M(z_1)| \neq 0$ for some positive integer M, where map F is defined by (1.1).

In fact, by calculating the inverse iterations of the fixed point z_0 twice, we have

$$\begin{cases} rx_1(1 - x_1) - bx_1y_1 = x_2, \\ dx_1y_1 = y_2, \end{cases} \tag{4.1}$$

and

$$\begin{cases} rx_2(1 - x_2) - bx_2y_2 = x^*, \\ dx_2y_2 = y^*. \end{cases} \tag{4.2}$$

Now a map F^2 has been constructed to map the point $z_1(x_1, y_1)$ to the fixed point $z_0(x^*, y^*)$ after two iterations if there are solutions different from z_0 for Eqs. (4.1) and (4.2).

From (4.2), one can get

$$rx_2^2 - rx_2 + \frac{by^*}{d} + x^* = 0. \tag{4.3}$$

By a simple calculation, we obtain that the equation (4.3) has one real root which is different from x^* denoted as

$$x_2 = 1 - \frac{1}{d}, \quad \text{for} \ \ d > 1, d \neq 2.$$

Substituting x_2 into (4.2), we get

$$y_2 = \frac{rd - r - d}{bd(d-1)}.$$

From (4.1), one can get

$$rx_1^2 - rx_1 + \frac{by_2}{d} + x_2 = 0. \tag{4.4}$$

If $d > 2$ and $r > \frac{4d^2}{d^2+d-2}$, then the equation (4.4) has two positive roots

$$x_{11} = \frac{rd^3 - rd^2 - d\sqrt{r(2 - 3d + d^2)(-2r + rd - 4d^2 + rd^2)}}{2(rd^3 - rd^2)},$$

$$x_{12} = \frac{rd^3 - rd^2 + d\sqrt{r(2 - 3d + d^2)(-2r + rd - 4d^2 + rd^2)}}{2(rd^3 - rd^2)}.$$

It is easy to check that $x_{12} \notin D_2$, so we get $x_1 = x_{11}$. Let $x_1 \in D_2$, i.e., $\bar{x}_1 < x_1 < \bar{x}_2$, which is equivalent to

$$(1 + \sqrt{1 - \frac{8}{rd}})^2 - (\frac{2\sqrt{(2 - 3d + d^2)(-2r + rd + rd^2 - 4d^2)}}{\sqrt{r}(d-1)d})^2 > 0 \qquad (4.5)$$

and

$$(\frac{2\sqrt{(2 - 3d + d^2)(-2r + rd + rd^2 - 4d^2)}}{\sqrt{r}(d-1)d})^2 - (1 - \sqrt{1 - \frac{8}{rd}})^2 > 0. \qquad (4.6)$$

Denote $q = \sqrt{1 - \frac{8}{rd}}$, and substitute q into (4.5) and (4.6), then we obtain

$$-2 + \frac{16}{d^2} + 2q + \frac{1 - 5d + 2d^2}{d - 1}(1 - q^2) > 0 \qquad (4.7)$$

and

$$2 - \frac{16}{d^2} + 2q - \frac{1 - 5d + 2d^2}{d - 1}(1 - q^2) > 0. \qquad (4.8)$$

From (4.7), we get

$$q_1 < q < q_2,$$

where

$$q_1 = \frac{-d + d^2 - 2\sqrt{(d - 2)(2 - 11d + 8d^2 + 3d^3 - 4d^4 + d^5)}}{d - 5d^2 + 2d^3},$$

$$q_2 = \frac{-d + d^2 + 2\sqrt{(d - 2)(2 - 11d + 8d^2 + 3d^3 - 4d^4 + d^5)}}{d - 5d^2 + 2d^3}.$$

From (4.8), we get

$$q < q_3 \quad \text{or} \quad q > q_4,$$

where

$$q_3 = \frac{d^2 - d^3 - 2\sqrt{(d - 2)(2 - 11d + 8d^2 + 3d^3 - 4d^4 + d^5)}}{d - 5d^2 + 2d^3},$$

$$q_4 = \frac{d - d^2 + 2\sqrt{(d - 2)(2 - 11d + 8d^2 + 3d^3 - 4d^4 + d^5)}}{d - 5d^2 + 2d^3}.$$

Notice that $q_3 < q_1 < 0 < q_4 < 1 < q_2$ for $d > 2$, and by the fact that $q = \sqrt{1 - \frac{8}{rd}} < 1$ for $rd > 8$, it follows that

$$0 < q_4 < q < 1,$$

which is equivalent to

$$r > \frac{2d(1 - 5d + 2d^2)^2}{(2 - 3d + d^2)(2 - 9d - d^2 + d^3) - (d - d^2)\sqrt{(d - 2)(2 - 11d + 8d^2 + 3d^3 - 4d^4 + d^5)}}. \qquad (4.9)$$

In addition, notice the relation $r > \frac{4d^2}{d^2 + d - 2}$, a direct computation yields:

$$\frac{2d(1 - 5d + 2d^2)^2}{(2 - 3d + d^2)(2 - 9d - d^2 + d^3) - (d - d^2)\sqrt{(d - 2)(2 - 11d + 8d^2 + 3d^3 - 4d^4 + d^5)}}$$

$$> \frac{4d^2}{d^2 + d - 2}.$$

Therefore, we obtain that if the conditions $d > 2$ and (4.9) hold, then $x_1 \in D_2$.

Substituting x_{11} into Eqs. (4.1), we have

$$y_1 = y_{11} = \frac{y_2}{dx_{11}} = \frac{2\sqrt{r}(r(d-1)-d)}{bd(\sqrt{r}d(d-1) - \sqrt{(2-3d+d^2)(r(d+d^2-2)-4d^2)})}.$$

Note that $|DF^2(x_1, y_1)| = r^2 d^2 (2x_1 - 1)(2x_2 - 1)x_1 x_2$. By some calculations, we get $|DF^2(x_1, y_1)| \neq 0$ if the conditions $d > 2$ and (4.9) are satisfied.

Obviously, if the conditions in Lemma 4.1 and the relations (4.9) are satisfied, then z_0 is a snap-back repeller in $U_r(z_0)$. Thus, the following theorem is established.

Theorem 4.1. *Assume that the conditions in Lemma 4.1 hold. If the conditions (4.9) are satisfied, then $z_0(x^*, y^*)$ is a snap-back repeller of system (1.1), and hence system (1.1) is chaotic in the sense of Marotto.*

Next, we give specific values of the parameters to show that the conditions in Lemma 4.1 and Theorem 4.1 can be realized.

Example 4.1. For $b = 2$, $d = 3.25$, $r = 4$, the system (1.1) has a positive fixed point $z_0(x^*, y^*) = (0.307692, 0.884615)$, and the eigenvalues associated with z_0 are $\lambda_{1,2} = 0.21875 \pm 1.220905i$. Based on Lemma 4.1 and Theorem 4.1, we find a region $U = \{(x,y)| \ 0.0949566 < x < 0.405043, \ \bar{y}_1 < y < \bar{y}_2\} \subset U_r(z_0) = \{(x,y)| \ x \in D_2, \ y \in D_3\}$ of z_0, and there exists a point $z_1(x_1, y_1) = (0.368629, 0.796049)$ satisfying that $F^2(z_1) = z_0$ and $|DF^2(z_1)| = -5.245553 \neq 0$, where

$$\bar{y}_1 = 2 - 2.375x - 0.5\sqrt{(52 - 104x)x},$$
$$\bar{y}_2 = 2 - 2.375x + 0.5\sqrt{(52 - 104x)x}.$$

Obviously z_0, $z_1 \in U$. Thus, z_0 is a snap-back repeller and system (1.1) is chaotic in the sense of Marotto.

Example 4.2. For $b = 2$, $d = 3.4$, $r = 4$, the system (1.1) has a positive fixed point $z_0(x^*, y^*) = (0.333333, 0.911765)$, and the eigenvalues associated with z_0 are $\lambda_{1,2} = 0.275000 \pm 1.253568i$. Based on Lemma 4.1 and Theorem 4.1, we find a region $U = \{(x,y)| \ 0.089578 < x < 0.410422, \ \bar{y}_1 < y < \bar{y}_2\} \subset U_r(z_0) = \{(x,y)| \ x \in D_2, \ y \in D_3\}$ of z_0, and there exists a point $z_1(x_1, y_1) = (0.367104, 0.304372)$ satisfying that $F^2(z_1) = z_0$ and $|DF^2(z_1)| = -5.245553 \neq 0$, where

$$\bar{y}_1 = 2 - 2.3x - 0.5\sqrt{(54.4 - 108.8x)x},$$
$$\bar{y}_2 = 2 - 2.3x + 0.5\sqrt{(54.4 - 108.8x)x}.$$

Obviously z_0, $z_1 \in U$. Therefore, z_0 is a snap-back repeller.

5. Numerical simulations

In this section, numerical simulations are given, including bifurcation diagrams, Lyapunov exponents (ML), fractal dimension (FD) and phase portraits, to illustrate the above theoretical analysis and to show new and more complex dynamic behaviors in the system (1.1).

The fractal dimension $[1, 2, 16, 24]$ is defined by using Lyapunov exponents as follows:

$$d_L = \begin{cases} 0 & \text{if no such } j \text{ exists,} \\ j + \frac{\sum_{i=1}^{i=j} L_i}{L_j} & \text{if } j < n, \\ n & \text{if } j = n, \end{cases}$$

with $L_1, L_2, \ldots, L_n$ being Lyapunov exponents, where j is the largest integer such that $\sum_{i=1}^{i=j} L_i \geq 0$ and $\sum_{i=1}^{i=j+1} L_i < 0$.

Our model is a two-dimensional map which has the fractal dimension in the form

$$d_L = 1 + \frac{L_1}{|L_2|}, \quad L_1 > 0 > L_2 \text{ and } L_1 + L_2 < 0.$$

5.1. Numerical Simulations for Stability and Bifurcations of Fixed Points

The following two cases are considered:

Case 1. Bifurcation diagram of system (1.1) in (d, x) plane for $1.5 \leq d \leq 1.7$, and $r = 3.5$ with initial value $(0.6, 0.2)$ is displayed in Fig. 1(a), which shows that there is a flip bifurcation (labeled "P-D") emerging from the fixed point $z_0(0.619048, 0.166667)$ with $d = 1.61538$, $\alpha_1 = 6.54545$ and $\alpha_2 = -183.273 < 0$.

Case 2. Bifurcation diagram of system (1.1) in (d, x) plane is given in Fig. 1(b) for $2.8 \leq d \leq 4.5$ and $r = 2.8$ with initial value $(0.3, 0.4)$. Fig. 1(b) exhibits Hopf bifurcation (labeled "HB"), which occurs at fixed point $z_0(0.321429, 0.45)$ and $d = 3.11111$ with $d_1 = 0.9 > 0$, $k = -1.51506 < 0$. Figs. 1(a) and 1(b) show the correctness of Theorems 3.1 and 3.2.
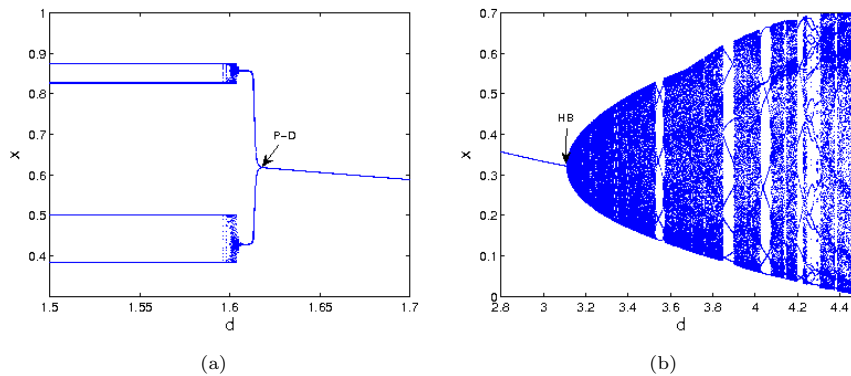

(a)   (b)

Figure 1. (a) Bifurcation diagram of map (1.1) in (d, x) plane for $r = 3.5$, $b = 2$, $d \in (1.5, 1.7)$, and the initial value is $(0.6, 0.2)$; (b) Bifurcation diagram of map (1.1) in (d, x) plane for $r = 2.8$, $b = 2$, $d \in (2.8, 4.5)$, and the initial value is $(0.3, 0.4)$.

5.2. Numerical Simulations for Marotto's Chaos

In this subsection, numerical simulations are shown for verifying the conditions in Theorem 4.1.

Case 1. By Example 4.1, the bifurcation diagram in (d, x) plane is plotted in Fig. 2(a) for $r = 4$, $b = 2$ and $d \in (3.1, 3.32)$ with initial value $(0.3, 0.8)$. The maximum Lyapunov exponents corresponding to (a) are computed as shown in Fig. 2(b). The Marotto's chaotic attractor is given in Fig. 2(c) for $d = 3.25$, which verifies Theorem 4.1.
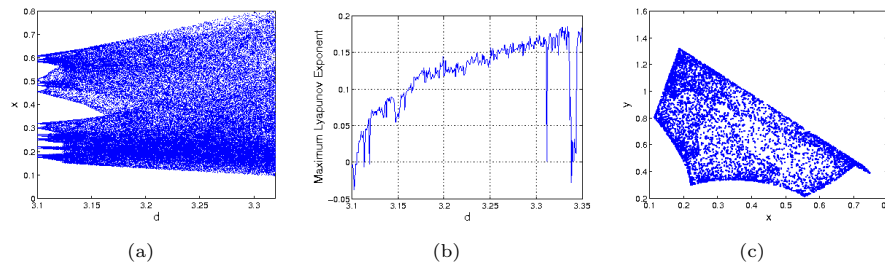

(a)   (b)   (c)

Figure 2. (a) Bifurcation diagram of map (1.1) in (d, x) plane for $r = 4$ and $d \in (3.1, 3.32)$ with initial value $(0.3, 0.8)$. (b) Maximum Lyapunov exponents corresponding to (a). (c) Chaotic attractor ($ML = 0.1489$, $FD = 2.35$) for $d = 3.25$ in (a).

Case 2. By Example 4.2, the bifurcation diagram in (d, x) plane is displayed in Fig. 3(a) for $r = 4$, $b = 2$ and $d \in (3.35, 3.45)$ with initial value $(0.3, 0.8)$. The maximum Lyapunov exponents corresponding to (a) are computed as shown in Fig. 3(b). The Marotto's chaotic attractor is given in Fig. 3(c) for $d = 3.4$. This shows the correctness of Theorem 4.1.
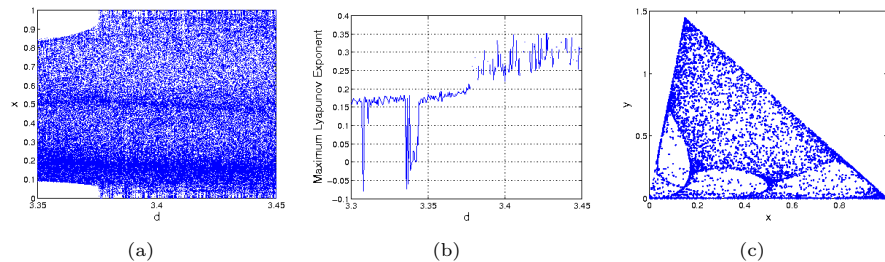

(a)   (b)   (c)

Figure 3. (a) Bifurcation diagram of map (1.1) in (d, x) plane for $r = 4$, $b = 2$ and $d \in (3.35, 3.45)$ with initial value $(0.3, 0.8)$. (b) Maximum Lyapunov exponents corresponding to (a). (c) Chaotic attractor ($ML = 0.2366$, $FD = 4.764$) for $d = 3.4$ in (a).

5.3. Further Numerical Simulations for the Map (1.1)

In this subsection, new and complex dynamical behaviors are investigated as the parameters vary.

The bifurcation diagrams in the two-dimensional plane are considered in the following four cases:

(i) Varying d in the range $0 \leq d \leq 4$ and fixing $r = 3.4$, $b = 2$;

(ii) Varying d in the range $0 \leq d \leq 4.1$ and fixing $r = 3.6$, $b = 2$;

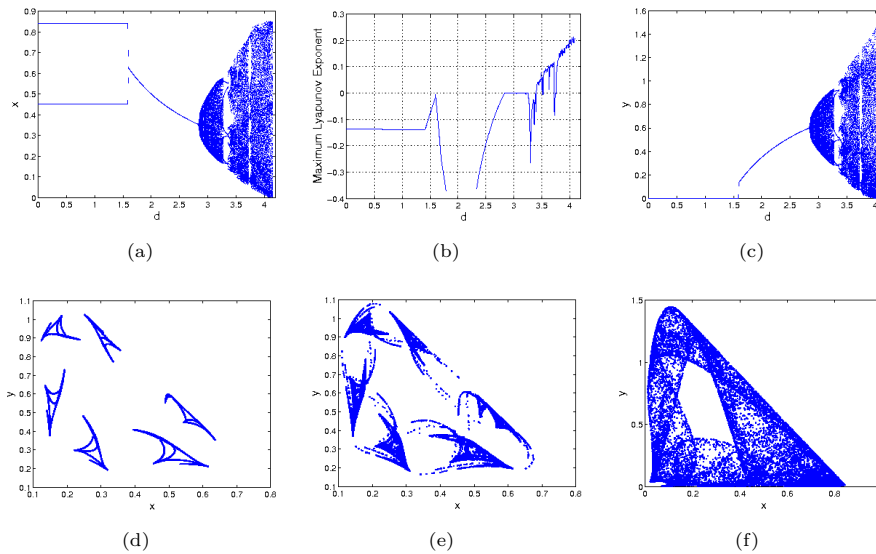(iii) Varying d in the range $2.4 \leq d \leq 3.2$ and fixing $r = 4.2$, $b = 2$;

Figure 4. (a) Bifurcation diagram of map (1.1) in (d, x) plane for $r = 3.4$ and $b = 2$. (b) Maximum Lyapunov exponents corresponding to (a). (c) Bifurcation diagram of map (1.1) in (d, y) plane for $r = 3.4$ and $b = 2$. (d-f) phase portraits for $d = 3.43, 4.46, 4.0$. (The maximum Lyapunov exponents and fractal dimensions corresponding are $ML = 0.08987, -0.02885, 0.2814$ and $FD = 1.352, 2.627, 4.53$ for Figs. 4(d)-(f), respectively.)

(iv) Varying r in the range $0 \le r \le 4.1$ and fixing $d = 3.5$, $b = 2$.

For case (i). The bifurcation diagrams of map (1.1) in (d, x) space and in (d, y) space for $r = 3.4$ and $b = 2$ are given in Figs. 4(a) and 4(c), respectively, which show the dynamical changes of the prey and predator as d varying. The maximum Lyapunov exponents corresponding to Fig.4(a) are computed in Fig. 4(b), confirming the existence of the chaotic regions and period orbits in the parametric space. From Figs. 4(a) and 4(c), we can see that a Hopf bifurcation occurs at $d \sim 2.8$ and an attracting invariant cycles bifurcates from the fixed point since $k = -0.354521$ and $d_1 = 0.847$ by Theorem 3.2. Furthermore, we observe the period-6, 18, 36, 8 windows within the chaotic regions and boundary crisis at $d = 4.1$. The phase portraits corresponding to Fig. 4(a) are shown in Figs. 4(d)-4(f) for showing six-coexisting chaotic attractors at $d = 3.43$ and 3.46, chaotic attractor at 4.0.

For case (ii). The bifurcation diagram of map (1.1) in (d, x) plane for $r = 3.6$ and $b = 2$ with initial value $(0.36, 0.65)$ is disposed in Fig. 5(a). The maximum Lyapunov exponents corresponding to Fig. 5(a) are given in Fig. 5(b), which show the existences of chaotic regions and period orbits as the parameter d varying. Figs. 5(a) and 5(b) clearly depict two onsets of chaos at $d = 0$ and $d \sim 3.195$, respectively, which are the crisis, and the non-attracting chaotic set at $d = 1.6$ and chaotic attractor at $d = 3.5$ are shown in Figs. 5(e) and 5(f), respectively. Fig. 5(c) is the bifurcation diagram in (d, y) plane for $r = 3.6$ and $b = 2$, which shows the dynamical changes of the predator as d varying. Comparing Figs. 5(a) and 5(c), we note that there are similar dynamics for $d \in (1.636, 4.1)$, but the predator tends to extinct(also see phase portrait Fig. 5(d)) when the prey is in chaotic dynamic for $d \in (0, 1.636)$.

For case (iii). The bifurcation diagram of map (1.1) in (d, x) plane for $r = 4.2$
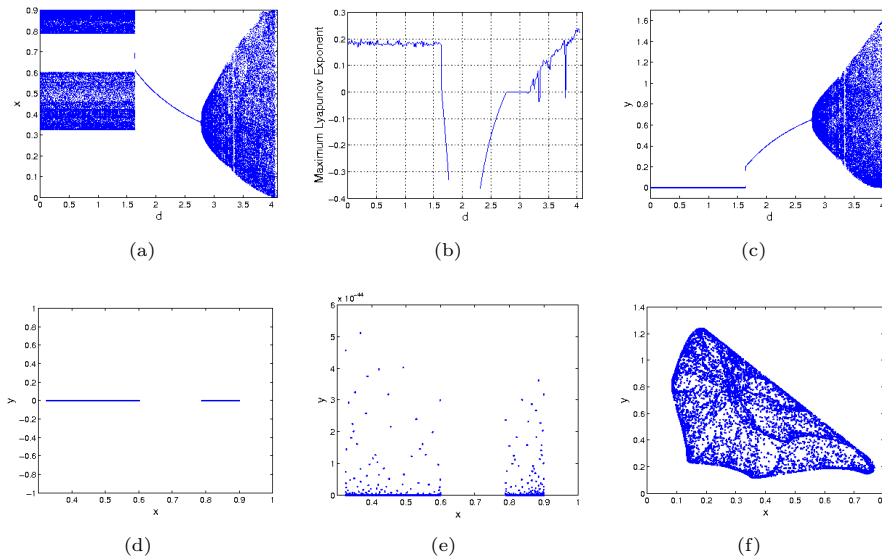
Figure 5. (a) Bifurcation diagram in (d, x) plane for $r = 3.6$ and $b = 2$. (b) Maximum Lyapunov exponents corresponding to (a). (c)Bifurcation diagram in (d, y) plane for $r = 3.6$ and $b = 2$. (d-f) Phase portraits for various values of d: (d) $d = 0.8$, (e) $d = 1.6$ and (f) $d = 3.5$.
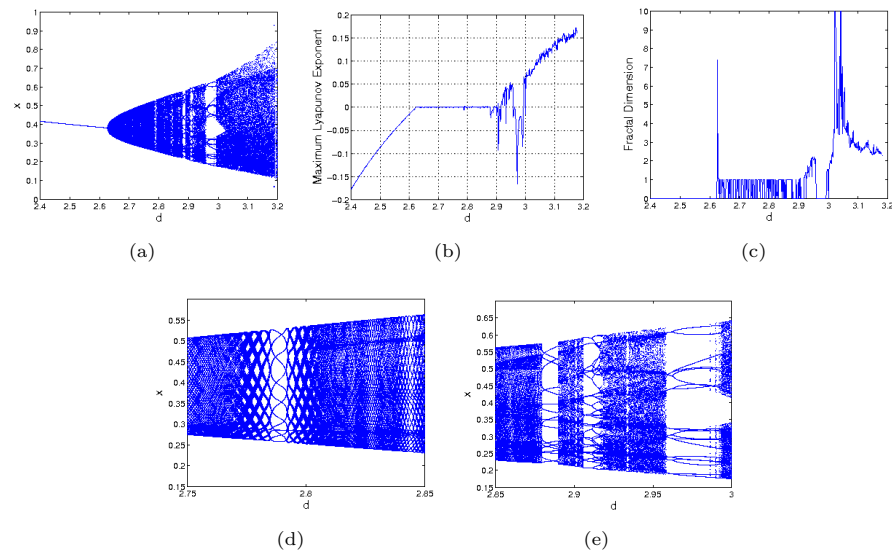

Figure 6. (a) Bifurcation diagram in (d, x) plane for $r = 4.2$ and $b = 2$. (b) Maximum Lyapunov exponents corresponding to (a). (c) Fractal dimensions corresponding to (a). Local amplification corresponding to (a) for: (d) $d \in (2.75, 2.85)$, (e) $d \in (2.85, 3.0)$.

and $b = 2$ with initial value $(0.38, 0.8)$ is shown in Fig. 6(a). Figs. 6(d) and 6(e) are the local amplifications for $d \in (2.75, 2.85)$ and $d \in (2.85, 3.0)$ in 6(a), respectively. The maximum Lyapunov exponents and fractal dimension corresponding to 6(a) are given in Figs. 6(b) and 6(c), respectively.

The diagrams show that there is a stable fixed point for $d \in (2.4, 2.625)$ and the fixed point loses its stability as d increases. Hopf bifurcation occurs at $d \sim 2.625$, and invariant circle appears as d increases and the invariant circle becomes to period-14 orbits at $d \sim 2.788$ suddenly. As the growth of d, quasi-periodic orbits appear, and the system undergoes period-doubling bifurcation to chaos with period-24 windows and interior crisis at $d \sim 2.91$ and period-10 windows and interior crisis at $d \sim 2.96$, respectively. Then, the chaotic behavior disappears at $d \sim 3.18$ suddenly. The phase portraits for various values of d are shown in Figs. 7(a)-7(i), which clearly depict how a smooth invariant circle bifurcates from the stable fixed point and an invariant circle to chaotic attractors. From Fig. 7 we observe that there are period-20, period-24, quasi-periodic orbits, six-coexisting chaotic attractors and attracting chaotic sets.
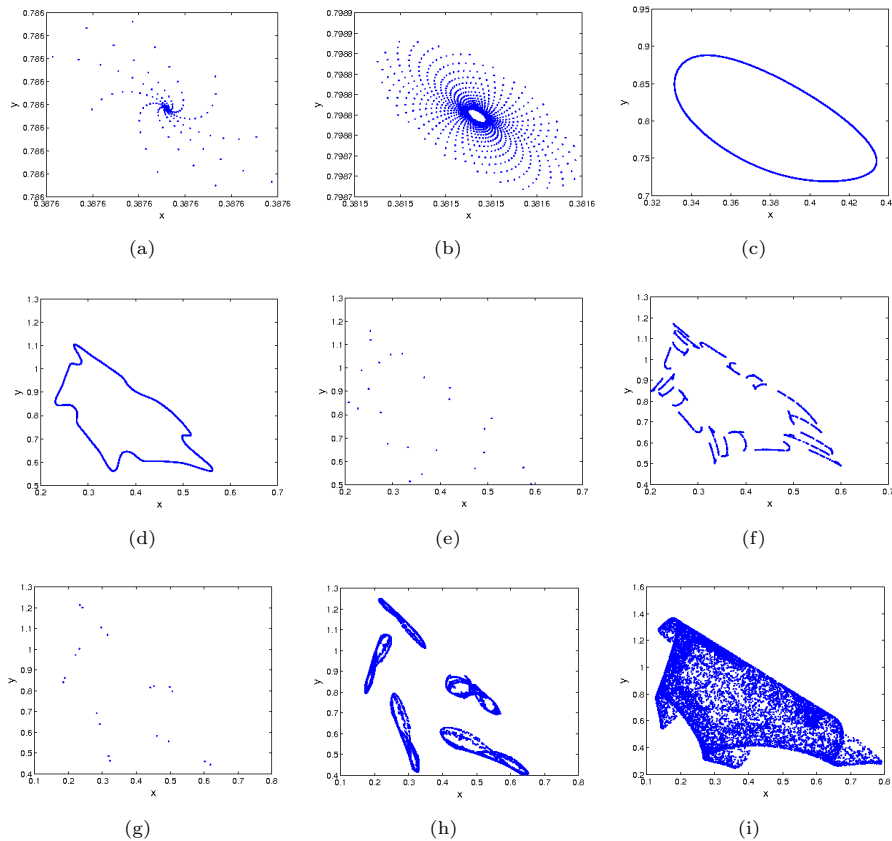

Figure 7. Phase portraits for various values of d corresponding to Fig. 6(a). (a) $d = 2.58$, (b) $d = 2.621$, (c) $d = 2.65$, (d) $d = 2.85$, (e) $d = 2.91$, (f) $d = 2.92$, (g) $d = 2.97$, (h) $d = 3.01$, (i) $d = 3.15$.(The Maximum Lyapunov exponents and fractal dimensions are $ML = 0.0059, 0.0685, 0.1525$ and $FD = 1.123, 1.867, 2.365$ for Figs. 7(f), (h), (i), respectively.)

For case (iv). The bifurcation diagram of map (1.1) in (r, x) plane for $d = 3.5$ and $b = 2$ with initial value $(0.28, 0.33)$ is shown in Fig. 8(a). Figs. 8(d) and 8(e) are the local amplifications for $r \in (2.65, 3.3)$ and $r \in (3.3, 3.6)$ in 8(a). The maximum Lyapunov exponents and fractal dimension corresponding to 8(a) are calculated and plotted in Figs. 8(b) and 8(c), respectively. For $r \in (3.2, 4.0)$, some

Lyapunov exponents are bigger than 0, some are smaller than 0, which implies that there exist stable fixed points or stable period windows in the chaotic region. The diagrams show that there is a stable fixed point for $r \in (1.5, 2.33)$ and the fixed point loses its stability as r increases. Hopf bifurcation occurs at $r \sim 2.33$, and invariant circle appears as r increases and the invariant circle suddenly becomes to period-7 orbits at $r \sim 2.719$ and period-13 orbits at $r \sim 3.11$. Furthermore, as the growth of r, we can observe the period-6, 7, 13, 14, 50 windows within the chaotic regions and boundary crisis at $r = 4.0$. The phase portraits for various values of r are revealed in Fig. 9.
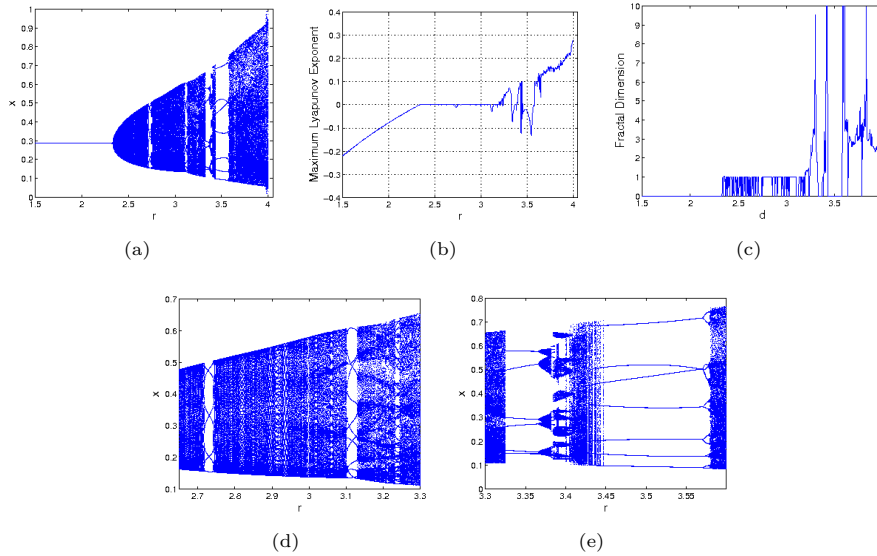

Figure 8. (a) Bifurcation diagram in (r, x) plane for $d = 3.5$ and $b = 2$. (b) Maximum Lyapunov exponents corresponding to (a). (c) Fractal dimensions corresponding to (a). (d-e) Local amplifications corresponding to (a) for $r \in (2.65, 3.3)$ and $r \in (3.3, 3.6)$.

6. Chaos control

In this section, we apply the state feedback control method [3, 9, 18] to stabilize chaotic orbits at an unstable fixed point of system (1.1).

Consider the following controlled form of system (1.1):

$$\begin{cases} x_{n+1} = rx_n(1 - x_n) - bx_ny_n + u_n, \\ y_{n+1} = dx_ny_n, \end{cases} \tag{6.1}$$

with the following feedback control law as the control force:

$$u_n = -k_1(x_n - x^*) - k_2(y_n - y^*),$$

where k_1 and k_2 are the feedback gains, (x^*, y^*) is the coexistence fixed point of system (1.1).
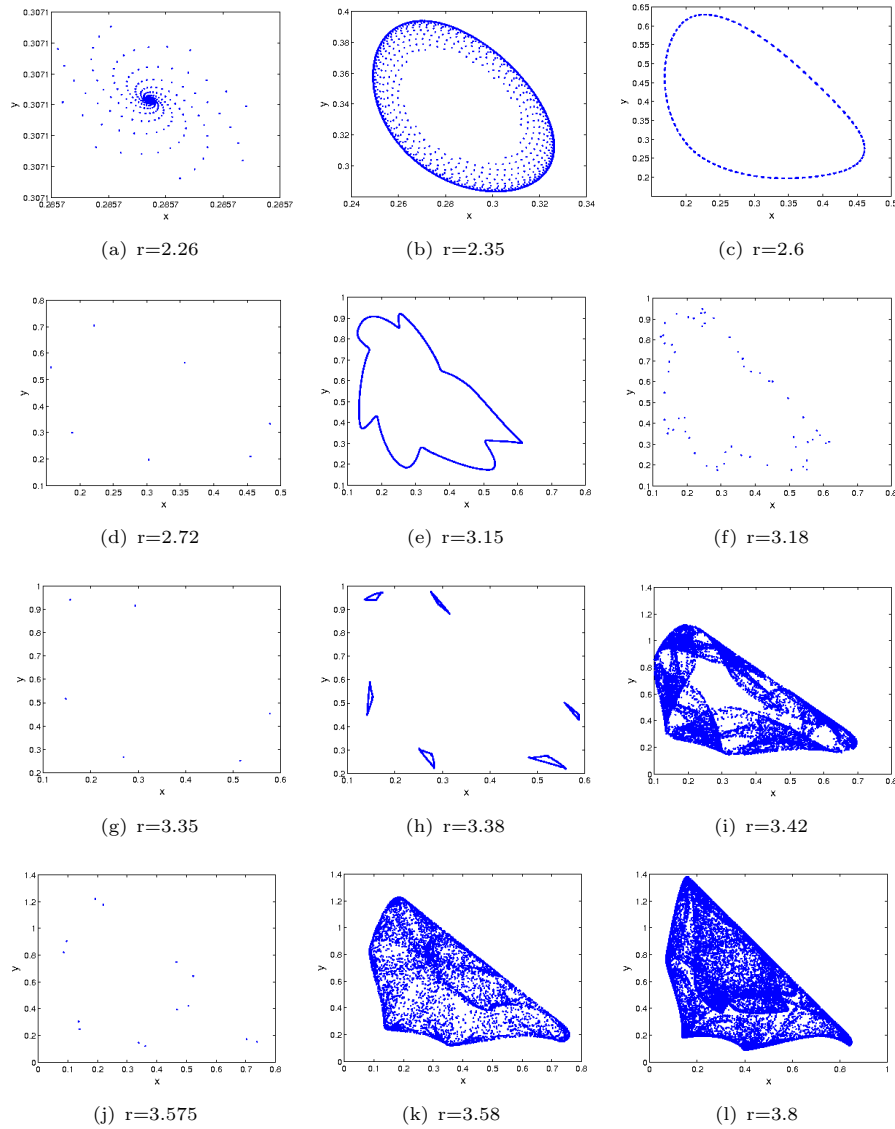
Figure 9. (a-l) Phase portraits for various values of r corresponding to Fig. 8(a).

The Jacobian matrix J of the controlled system (6.1) evaluated at the fixed point (x^*, y^*) is given by

$$J(x^*, y^*) = \begin{pmatrix} r - 2rx^* - by^* - k_1 & -bx^* - k_2 \\ dy^* & dx^* \end{pmatrix},$$

and the characteristic equation of the Jacobian matrix $J(x^*, y^*)$ is

$$\lambda^2 - (r + (d - 2r)x^* - by^* - k_1)\lambda + d((r - k_1)x^* - 2rx^{*2} + k_2 y^*) = 0.$$

Assume that the eigenvalues are given by λ_1 and λ_2, then

$$\lambda_1 + \lambda_2 = r + (d - 2r)x^* - by^* - k_1 \tag{6.2}$$

and

$$\lambda_1 \lambda_2 = d((r - k_1)x^* - 2rx^{*2} + k_2 y^*). \tag{6.3}$$

The lines of marginal stability are determined by the equations $\lambda_1 = \pm 1$ and $\lambda_1 \lambda_2 = 1$. These conditions guarantee that the eigenvalues λ_1 and λ_2 have modulus are equal to 1.

Assume that $\lambda_1 \lambda_2 = 1$, then from (6.3) we have $l_1 : bdk_1 - d(d(r-1) - r)k_2 = br(d-2) - bd$.

Assume that $\lambda_1 = 1$, then from (6.2), (6.3) we get $l_2 : k_2 = -\frac{b}{d}$.

Assume that $\lambda_1 = -1$, then from (6.2), (6.3) we obtain $l_3 : 2bdk_1 - d(d(r-1) - r)k_2 = b(d(3+r) - 3r)$.

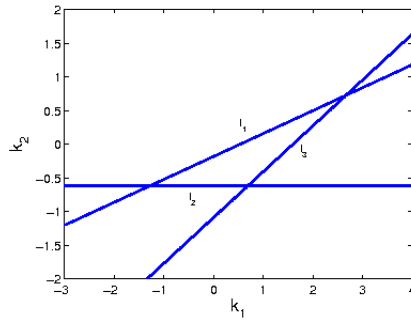The stable eigenvalues lie within a triangular region by lines l_1, l_2 and l_3 (see Fig. 10).

Figure 10. The bounded region for the eigenvalues of the controlled system (6.1) in the (k_1, k_2) plane for $r = 4.2$, $d = 3.15$ and $b = 2$.
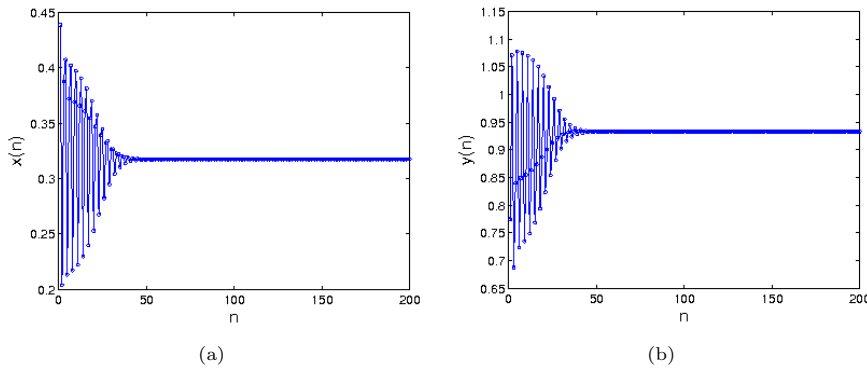

Figure 11. (a) The time responses for the state x of the controlled system (6.1) in the (n, x) plane for $r = 4.2$, $d = 3.15$, $b = 2$, $k_1 = 1.5$, $k_2 = 0.2$. The initial value is $(0.3, 0.82)$. (b) The time responses for the state y of the controlled system (6.1) in the (n, y) plane.

Some numerical simulations have been performed to see how the state feedback method controls the unstable fixed point. Parameter values are fixed as $r = 4.2$,

$d = 3.15$, $b = 2$. The initial value is $(0.3, 0.82)$, and the feedback gains $k_1 = 1.5$, $k_2 = 0.2$. It is shown in Fig. 11 that a chaotic trajectory is stabilized at the fixed point $(0.31746, 0.93333)$.

7. Conclusions

In this paper, we investigated the complex dynamic behaviors of the predator-prey system (1.1) as a discrete-time dynamical system, and showed that the unique coexistence fixed point of system (1.1) can undergo flip bifurcation and Hopf bifurcation. Moreover, system (1.1) displays much more interesting dynamical behaviors, which include orbits of period-6, 7, 8, 10, 14, 18, 24, 36, 50, invariant cycles, quasi-periodic orbits and chaotic sets, in particular, Marotto's chaotic attractors. They all imply that the predator and prey can coexist at period-n oscillatory balance behaviors or a oscillatory balance behavior, but the predator-prey system are unstable if chaotic behavior occurs, and particularly, the predator will ultimately tend to extinct, or tend to a stable fixed point if the prey is in chaotic. These results show far richer dynamics of the discrete-time model. Specifically, we have stabilized the chaotic orbits at an unstable fixed point using the feedback control method.

Acknowledgements

References

[1] K. T. Alligood, T. D. Sauer and J. A. Yorke, *Chao-An Introduction to Dynamical Systems*, New York, Springer-Verlag, 1996.

[2] J. H. E. Cartwright, *Nonlinear stiffness, Lyapunov exponents, and attractor dimension*, Phys. Lett. A., 1999, 264, 298–302.

[3] G. Chen and X. Dong, *From Chaos to Order: Perspectives, Methodologies, and Applications*, World Scientific, Singapore, 1998.

[4] X. W. Chen, X. L. Fu and Z. J. Jing, *Dynamics in a discrete-time predator-prey system with Allee effect*, Acta. Math. Appl. Sin., 2012, 29, 143–164.

[5] X. W. Chen, X.L. Fu and Z. J. Jing, *Complex dynamics in a discrete-time predator-prey system without Allee effect*, Acta. Math. Appl. Sin., 2018, 29, 355–76.

[6] Z. Cheng, Y. Lin and J. Cao, *Dynamical behaviors of a partial-dependent predator-prey system*, Chaos, Solit. Fract., 2006, 28, 67–75.

[7] S. R. Choudhury, *On bifurcations and chaos in predator-prey models with delay*, Chaos, Solit. Fract., 1992, 2, 393–409.

[8] M. Danca, S. Codreanu and B. Bakó, *Detailed Analysis of a Nonlinear Prey-predator Model*, Journal of Biological Physics, 1997, 23, 11–20.

[9] S. Elaydi, *An Introduction to Difference Equations, 3rd ed.*, Springer-Verlag, New York, 2005.

[10] S. Elaydi, *Discrete Chaos: With Applications in Science and Engineering, 2nd ed*, Chapman and Hall/CRC, BocaRaton, FL, 2008.

[11] M. Fan and S. Agarwal, *Periodic solutions of nonautonomous discrete predator-prey system of Lotka-Volterra type*, Appl Anal., 2002, 81, 801–812.

[12] J. Guckenheimer and P. Holmes, *Nonlinear oscillations, dynamical systems and bifurcations of vector fields*, New York, Springer-Verlag, 1983.

[13] D. P. Hu and H. J. Cao, *Bifurcation and chaos in a discrete-time predator-prey system of Holling and Leslie type*, Commun Nonlinear Sci Numer Simulat, 2015, 22, 702–715.

[14] G. Jiang and Q. Lu, *Impulsive state feedback of a predator-prey model*, J. Comput. Appl. Math., 2007, 200, 193–207.

[15] G. Jiang, Q. Lu and L. Qian, *Complex dynamics of a Hollingtype II prey-predator system with state feedback control*, Chaos, Solit. Fract., 2007, 31, 448–461.

[16] J. L. Kaplan and J. A Yorke, *Aregime observed in a fluid flow model of Lorenz*, Comm. Math. Phys., 1979, 67, 93–108.

[17] B. Liu, Z. Teng and L. Chen, *Analysis of a predator-prey model with Holling II functional response concerning impulsive control strategy*, J. Comput. Appl. Math., 2006, 193, 347–362.

[18] S. Lynch, *Dynamical Systems with Applications Using Mathematica*, Birkhäser, Boston, 2007.

[19] X. Liu and D. Xiao, *Complex dynamic behaviors of a discrete-time predator-prey system*, Chaos, Solit. Fract., 2007, 32, 80–94.

[20] F. R. Marotto, *Snap-back repeller imply chaos in $\mathbb{R}^n$*, J. Math. Anal. Appl., 1978, 63, 199–223.

[21] F. R. Marotto, *On redefining a snap-back repeller*, Chaos, Solit. Fract., 2005, 25, 25–28.

[22] J. D. Murray, *Mathematical Biology*, New York, Springer-Verlag, 1993.

[23] M. Martelli, *Discrete Dynamical Systems and Chaos*, Pitman monographs and surveys in pure and applied mathematics, New York, Longman, 1992.

[24] E. Ott, *Chaos in Dynamical Systems, 2nd ed*, Cambridge, Cambridge University Press, 2002.

[25] C. Sun, M. Han, Y. Lin and Y. Chen, *Global qualitative analysis for a predator-prey system with delay*, Chaos, Solit. Fract., 2007, 32, 1582–1596.

[26] V. Volterra, *Lecons sur la Théorie Mathématique de la Lutte pour la Vie*, Paris, Gauthier-Villars, Reissued 1931.

[27] S. Winggins, *Introduction to Applied Nonlinear Dynamical System and Chaos*, New York, Springer-Verlag, 1990.